TECHNICAL ARTICLE

Structural and optical properties of Ba(Co₁₋ₓZnₓ)SiO₄ ($x = 0.2, 0.4, 0.6, 0.8$)

J. Anike,[1] R. Derbeshi,[2] W. Wong-Ng,[3,a)] W. Liu,[4] D. Windover,[3] N. King,[3] S. Wang,[5] J. A. Kaduk [ID],[6,7] and Y. Lan[2]

[1]*Mechanical Engineering Department, Catholic University of America, Washington DC 20060, USA*

[2]*Physics Department, Morgan State University, Baltimore, MD 21251, USA*

[3]*Material Measurement Laboratory, National Institute of Standards and Technology, Gaithersburg, MD 20899, USA*

[4]*Physics Department, Tianjin University, Tianjin, China*

[5]*Physics Department, Tianjin Normal University, Tianjin, China*

[6]*Department of Chemistry, Illinois Institute of Technology, Chicago, IL 60616, USA*

[7]*Department of Physics, North Central College, Naperville IL 60540, USA*

Structural characterization and X-ray reference powder pattern determination have been conducted for the Co- and Zn-containing tridymite derivatives Ba(Co₁₋ₓZnₓ)SiO₄ ($x = 0.2, 0.4, 0.6, 0.8$). The bright blue series of Ba(Co₁₋ₓZnₓ)SiO₄ crystallized in the hexagonal $P6_3$ space group (No. 173), with $Z = 6$. While the lattice parameter "a" decreases from 9.126 (2) Å to 9.10374(6) Å from $x = 0.2$ to 0.8, the lattice parameter "c" increases from 8.69477(12) Å to 8.72200(10) Å, respectively. Apparently, despite the similarity of ionic sizes of Zn^{2+} and Co^{2+}, these opposing trends are due to the framework tetrahedral tilting of $(ZnCo)O_4$. The lattice volume, V, remains comparable between 626.27 Å³ and 626.017 (7) Å³ from $x = 0$ to $x = 0.8$. UV-visible absorption spectrum measurements indicate the band gap of these two materials to be ≈3.3 and ≈3.5 eV, respectively, therefore potential UV photocatalytic materials. Reference powder X-ray diffraction patterns of these compounds have been submitted to be included in the Powder Diffraction File (PDF). © *2019 International Centre for Diffraction Data.* [doi:10.1017/S0885715619000447]

Key words: Reference powder X-ray diffraction patterns, crystal structure, stuff tridymite derivatives, Ba(Co₁₋ₓZnₓ)SiO₄ ($x = 0.2, 0.4, 0.6, 0.8$), Powder Diffraction File, UV-visible spectrum

I. INTRODUCTION

The continuing demands for environmentally friendly alternative energy technologies have led to greatly increased research into energy sustainability. In recent years production of clean-burning hydrogen fuel has gained intensified attention as oil and other nonrenewable fuels become increasingly depleted and expensive. Methods such as photocatalytic water splitting are being investigated to produce hydrogen. Photocatalysis is a type of catalysis that results in the modification of the rate of a photoreaction (a chemical reaction that involves the absorption of light by one or more reacting species such as semiconductors) by adding catalysts that participate in the chemical reaction without being consumed.

Despite considerable global efforts, commercialization of photocatalysis technology, as compared to the photovoltaic technology (Paranthaman *et al.*, 2015), has encountered setbacks due to the difficulties of obtaining efficient materials. Much current research is focusd on material improvements of semiconductors that have narrow bandgaps of about 2.5 eV, which is one of the requirements for effective photocatalysis materials in the visible light regime (Abe, 2010; Maeda, 2011; Osterloh, 2013; Khan *et al.*, 2015; Martsinovich, 2016; King *et al.*, 2017). Oxide materials including silicates exhibit potentials to be photocatalysis materials. In this paper, we focus our efforts on a silicate series of compounds, which is tridymite (SiO₂)-related.

Alkaline earth silicates have been known to possess stable crystal structure, high physical and chemical stability and to function as effective luminescent hosts (Barry, 1968; Jüstel *et al.*, 1998; Yao *et. al.*, 2011; Streit *et al.*, 2013; Lin *et al.*, 2017 and Nagai *et al.*, 2015). Tridymite is a high-temperature polymorph of silica that usually occurs as white or colorless pseudo-hexagonal crystals. By partially replacing Si^{4+} ions with other tetrahedrally coordinated ions of lower valence ions such as Zn^{2+} and Co^{2+}, and by substituting the large ions, such as Ba^{+2} into the tetrahedral framework, the resulting compounds Ba*M*SiO₄ (*M* = Co and/or Zn) would maintain charge balance. Therefore, Ba*M*SiO₄ belong to a large structural family of stuffed tridymite derivatives (Taniguschi *et al.*, 2014). BaCoSiO₄ has been reported to have a theoretically narrow band gap of about 2 eV (Taniguschi *et al.*, 2014).

There are three goals in this paper. Firstly, the structure of Ba(Co₁₋ₓZnₓ)SiO₄ ($x = 0.2, 0.4, 0.6, 0.8$) compounds are investigated for the effect of Zn substitution on the Co site. The second goal is to obtain band gap values of these materials by measuring their UV-visible absorption spectra. Lastly, since X-ray diffraction is a non-destructive technique, X-ray diffraction patterns are especially important for phase characterization, therefore the third goal of this investigation was to determine experimental powder reference X-ray patterns (McMurdie *et al.*, 1986a and 1986b) for the Ba(Co₁₋ₓZnₓ)

a)Author to whom correspondence should be addressed. Electronic mail: winnie.wong-ng@nist.gov

SiO$_4$ series and to make them available through submission to the Powder Diffraction File (PDF, 2018).

II. EXPERIMENTAL

A. Sample preparation

The starting stoichiometric chemicals BaCO$_3$, Co$_3$O$_4$, ZnO and SiO$_2$ were weighed, mixed and pelletized to form Ba(Co$_{1-x}$Zn$_x$)SiO$_4$ ($x = 0.2$, 0.4, 0.6, 0.8). The pellets were heat-treated in a furnace at 850 °C for 24 h, 900 °C for 40 h, 1000 °C for 52 h, 1100 °C for 60 h and at 1200 °C for another 60 h. Between each heat treatment, the samples were furnace cooled, ground and re-pelletized. The heat treatment process was repeated until no further changes were detected in the powder X-ray diffraction patterns.

B. Estimation of composition using X-ray fluorescence

The estimation of composition for sample Ba(Zn$_{0.4}$Co$_{0.6}$)SiO$_4$ was performed on a Bruker M4 Tornado micro X-ray fluorescence instrument. A Rh X-ray source, set to 50 kV and 300 uA, with a 20 um mono-capillary were used for excitation (S.N. 2001495). A Bruker XFlash 450 um thick, Silicon Drift Detector (S.N. 11881_0239) was used for data collection for two scans, with a live time of 300s per scan. Each spectrum used a minimum peak sum of over 100 k X-ray counts per analyzed element, eliminating counting statistics as a source of uncertainty. Analysis were performed using Bruker Quantify version 1.3.1.3327 with standard Spectrum Elements method and calibrated for our instrument (S.N. 6099).

C. X-ray rietveld refinements and reference powder X-ray diffraction patterns

Powder X-ray diffraction was used to investigate phase purity and establish phase relationships. These experiments were carried out using a Phillips X-ray powder diffractometer with Cu K$_\alpha$ radiation and equipped with a series of soller slits and a scintillation counter. (The purpose of identifying the equipment in this article is to specify the experimental procedure. Such identification does not imply recommendation or endorsement by the National Institute of Standards and Technology.) The 2θ scanning range was from 10° to 79°, with step intervals of 0.03°. The reference diffraction pattern of the BaCoSiO$_4$ phase (International Centre for Diffraction Data/Powder Diffraction file (PDF4+, 2019)) was used for performing phase identification.

For structure analysis, the Ba(Co$_{1-x}$Zn$_x$)SiO$_4$ ($x = 0.2$, 0.4, 0.6, and 0.8) compounds were packed into 0.3 mm glass capillaries. The powder patterns were measured on a PANalytical Empyrean diffractometer equipped with an incident-beam focusing mirror and an X'Celerator detector. The patterns (1–100° 2θ, 0.0167113° steps, 4 s/step, 1/4° divergence slit, 0.02 radian Soller slits) were measured using Mo K$_\alpha$ radiation. The Rietveld refinement technique (Rietveld, 1969) with software suite GSAS (Larson and von Dreele, 2004) was used to determine the structure of Ba(Co$_{1-x}$Zn$_x$)SiO$_4$ ($x = 0.2$, 0.4, 0.6, and 0.8) using BaCoSiO$_4$ (PDF4+, 4-22-3559) as an initial model for refinement. Using X-ray fluorescence method, we have performed composition

determination on one sample, namely, Ba(Zn$_{0.4}$Co$_{0.6}$)SiO$_4$. The ratio of Zn/Co was indeed determined to be 4/6 (discussed later). The result indicated that neither species has significantly vaporized, and no impurity phases were expected nor observed, and thus the synthesized chemistry is expected to be close to the intended chemistry. Therefore, in the refinement models of all four samples, the site occupancy factors were fixed to be exactly as synthesized.

Reference powder X-ray diffraction patterns were obtained with a Rietveld pattern decomposition technique. Using this technique, the reported peaks were derived from the extracted integrated intensities, and positions calculated from the lattice parameters. When peaks are not resolved at the resolution function, the intensities are summed, and an intensity-weighted d-spacing is reported.

D. Band gap measurements

The optical properties of the synthesized Ba(Co$_{1-x}$Zn$_x$)SiO$_4$ ($x = 0$, 0.2, 0.8, and 1.0) compounds were investigated by measuring the UV-visible absorption spectra. The synthesized pellets were ground and suspended in deionized-water for UV-visible measurements. The UV-visible optical absorption spectra of the suspensions were measured for one minute using a DU 640 spectrophotometer with wavelength range of 200 to 1100 nm.

E. Bond Valence Sum (BVS) calculations

Bond valence sum (BVS) values for the Ba, Co, Zn, and Si sites were calculated using the Brown-Altermatt empirical expression (Brown and Altermatt, 1985; and Brese and O'Keeffe, 1991). The BVS of an atom i is defined as the sum of the bond valences v_{ij} of all the bonds from atoms i to atoms j. The most commonly adopted empirical expression for the bond valence v_{ij} as a function of the interatomic distance d_{ij} is $v_{ij} = \exp[(R_0 - d_{ij})/B]$. The parameter, B, is commonly taken to be a "universal" constant equal to 0.37 Å. The values used for the reference distance R_0 for Ba^{2+}-O, Zn^{2+}-O, Co^{2+}-O, Si^{4+}-O are 2.29, 1.920, 1.911, 1.624 Å, respectively (Brown and Altermatt, 1985; and Brese and O'Keeffe, 1991). When more than one atom types occupy the same site, the resulting BVS is the weighted sum of each site occupancy.

III. RESULTS AND DISCUSSION

A. Structure characterization

The Rietveld refinement results including the refinement R values and goodness of fit for each sample of the Ba(Co$_{1-x}$Zn$_x$)SiO$_4$ ($x = 0.2$, 0.4, 0.6, and 0.8) series are given in Table I. Figure 1 illustrates the observed (crosses), calculated (solid line), and difference XRD patterns (bottom) for

TABLE I. Rietveld refinement residuals for Ba(Co$_{1-x}$Zn$_x$)SiO$_4$ ($P6_3$ (No. 173), $Z = 6$).

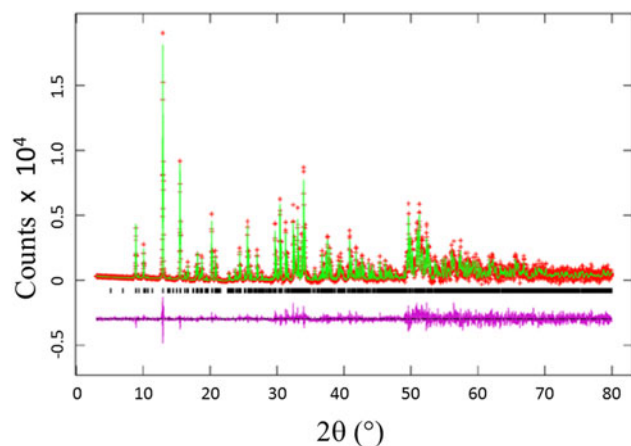| Composition	R_{wp}	R_p	χ^2
Ba(Co$_{0.8}$Zn$_{0.2}$)SiO$_4$ ($x = 0.2$)	0.0637	0.0840	1.92
Ba(Co$_{0.6}$Zn$_{0.4}$)SiO$_4$ ($x = 0.4$)	0.0905	0.0711	1.75
Ba(Co$_{0.4}$Zn$_{0.6}$)SiO$_4$ ($x = 0.6$)	0.0733	0.0924	2.27
Ba(Co$_{0.2}$Zn$_{0.8}$)SiO$_4$ ($x = 0.8$)	0.0733	0.0918	2.27

Figure 1. (Colour online) Observed (crosses), calculated (solid line), and difference XRD pattern (bottom) for $Ba(Co_{0.6}Zn_{0.4})SiO_4$ by Rietveld analysis technique. The difference pattern is plotted at the same scale as the other calculated peak positions up to 50° 2θ. At higher angles, the scale has been magnified five times.

Figure 2. Plot of unit cell parameter, a and c of $Ba(Co_{1-x}Zn_x)SiO_4$ vs. x. A monotonic increase of a and decrease of c are observed.

$Ba(Co_{1-x}Zn_x)SiO_4$. The difference pattern is plotted at the same scale as the other patterns. Above 50° 2θ, the vertical scale has been magnified five times. The row of tick marks indicates the calculated peak positions.

Table II lists the lattice parameters for $Ba(Co_{1-x}Zn_x)SiO_4$ ($x = 0$, 0.2, 0.4, 0.6, and 0.8). This series of compounds, having the hexagonal space group of $P6_3$, are isostructural. Lattice parameters of Liu and Barbier (1993) were used for comparison (Table II). As the Shannon ionic radii for Co^{2+} (C.N. of 4) and Zn^{2+} are close to each other (0.58 vs. 0.6 Å) (Shannon, 1976), one does not expect the unit cell volumes of the $Ba(Co_{1-x}Zn_x)SiO_4$ members to differ significantly from each other. In Figure 2, it is interesting to see the length of the a axis decreases from $Ba(Co_{0.8}Zn_{0.2})SiO_4$ to $Ba(Co_{0.2}Zn_{0.8})SiO_4$ (from 9.126 (2) to 9.10374(6) Å), respectively, but the c-axis increases from $Ba(Co_{0.8}Zn_{0.2})SiO_4$ to $Ba(Co_{0.2}Zn_{0.8})SiO_4$ (from 8.69477(12) Å to 8.72200(10) Å), resulting in rather similar unit cell volume in the series (unit cell volume varies between 626.3 Å^3 and 626.0 Å^3). There is also a trend of increasing density as the x value increases.

Table III gives the coordinates of the atomic sites of $Ba(Co_{1-x}Zn_x)SiO_4$. The structure is confirmed to be that of a Ba-stuffed tetrahedral tridymite framework. The structure consists of alternating 6-membered rings of corner-shared SiO_4 and the relatively larger $(Co/Zn)O_4$ tetrahedra. Six of these tetrahedra enclose six-fold channels along the c-direction. All rings are similar with an almost triangular shape and are stacked along the c-direction, joined via the O10 sites in a staggered manner. The Co/Zn and Si sites are ordered, with the larger $(Co/Zn)O_4$ tetrahedra pointing upward and smaller
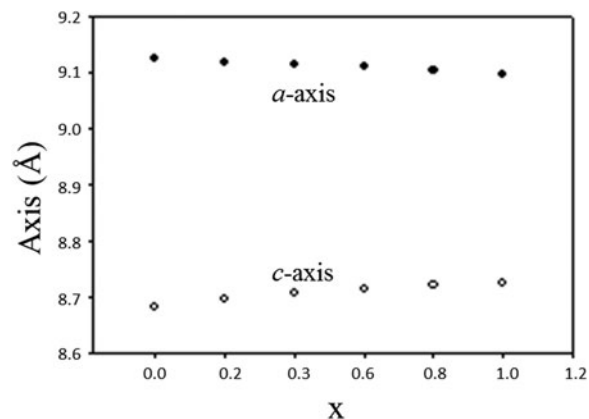
SiO_4 pointing downward. The ordered structure is likely due to the large differences in the formal ionic valences of $(Co/Zn)^{2+}$ vs. Si^{4+} and in bond lengths (1.86(3) Å to 2.06(4) Å for (Co/Zn)-O and 1.53(3) Å to 1.67 Å for Si-O). Figures 3 and 4 show corner-shared SiO_4 and the larger $(Co/Zn)O_4$ tetrahedra along the ab plane. Figure 5 illustrates the Ba polyhedra. Figure 6 shows the 6-membered rings with Ba atoms in the channels viewed along the c-axis, and it also gives the atomic labeling.

There are three crystallographically different six-fold channels filled with Ba atoms (Ba1, Ba2, and Ba3). These three Ba sites are all located on threefold axes, however, with different coordination characteristics. As shown in Table IV, while Ba1 and Ba2 sites are both 9-fold coordinated (six short Ba-O7 plus three long Ba-O10 bonds (3.04 Å) for Ba1, three short Ba-O8 and three short Ba-O10 plus three long Ba-O9 bonds (3.01 Å) for Ba2), Ba3 is only 6-fold coordinated (three short Ba-O8 and three short Ba-O9 bonds). The smaller coordination number for Ba3 is because O10 site is displaced significantly from Ba3, giving rise to the Ba3-O separation of >3.5 Å. Because of this large separation, we would expect the displacement factor for Ba3 to be larger as compare to those of Ba1 and Ba2.

Judging from the average (Co, Zn)-O distances in these compounds, there is a small decrease from 1.98 to 1.95 Å from $x = 0.2$ to 0.8, which is the probable cause of the decreasing a-axis cell parameters, whereas the slightly increasing Ba-O distances in the series resulted in the increasing trend of the c-axis. The displacement of the O10 site corresponds to the collapse of the tetrahedral framework around the Ba atoms, involving the tilting of $(Co/Zn)O_4$ and SiO_4 tetrahedra around horizontal axes that is approximately parallel to the [110] direction (Liu and Barbier, 1993). Taking Ba1 as the

TABLE II. Cell parameters for $Ba(Co_{1-x}Zn_x)SiO_4$ ($x = 0$ to 1), space group $P6_3$ (No. 173), $Z = 6$, and d_{cal} represents calculated density.

Chemical formula	a (Å)	c (Å)	V (Å)	d_{cal} (g/cm^3)	References
$BaCoSiO_4$	9.126 (2)	8.683 (4)	626.3 (5)	4.587	(PDF4+ 04-11-3559)
$Ba(Co_{0.8}Zn_{0.2})SiO_4$	9.11878 (7)	8.69477 (12)	626.127 (11)	4.609	This work
$Ba(Co_{0.6}Zn_{0.4})SiO_4$	9.11386 (8)	8.70614 (13)	626.269 (11)	4.628	This work
$Ba(Co_{0.4}Zn_{0.6})SiO_4$	9.10920 (7)	8.71363 (12)	626.167 (10)	4.650	This work
$Ba(Co_{0.2}Zn_{0.8})SiO_4$	9.10374 (6)	8.72200 (10)	626.017 (7)	4.671	This work
$BaZnSiO_4$	9.0955 (5)	8.7251 (9)	625.11 (7)	4.698	(Liu & Barbier, 1993)

TABLE III. Atomic coordinates and displacement factors for compounds for $Ba(Co_{1-x}Zn_x)SiO_4$ $P6_3$ (No. 173), $Z = 6$.

Atom	x	y	z	Site Occ.	U_{iso}	Wyckoff symbol
(1) $Ba(Co_{0.8}Zn_{0.2})SiO_4$ ($x = 0.2$)						
Ba1	0.0	0.0	0.25 (0)	1.0	0.0030 (9)	2
Ba2	0.33333	0.66667	0.2272 (7)	1.0	0.0124 (13)	2
Ba3	0.66667	0.33333	0.2177 (0)	1.0	0.031 (2)	2
Co4/Zn5	0.6812 (9)	0.6736 (12)	0.5352 (11)	0.8/0.2	0.01	6
Si6	0.669 (2)	−0.004 (3)	0.432 (2)	1.0	0.005	6
O7	0.747 (3)	0.909 (4)	0.523 (3)	1.0	0.005	6
O8	0.467 (4)	0.897 (3)	0.483 (3)	1.0	0.005	6
O9	0.765 (4)	0.191 (4)	0.453 (3)	1.0	0.005	6
O10	0.716 (3)	0.654 (3)	0.762 (2)	1.0	0.005	6
(2) $Ba(Co_{0.6}Zn_{0.4})SiO_4$ ($x = 0.4$)						
Ba1	0.0	0.0	0.244 (2)	1.0	0.0005 (12)	2
Ba2	0.33333	0.66667	0.220 (3)	1.0	0.007 (2)	2
Ba3	0.66667	0.33333	0.2180 (1)	1.0	0.025 (2)	2
Co4/Zn5	0.675 (2)	0.670 (2)	0.528 (2)	0.6/0.4	0.01	6
Si6	0.661 (4)	−0.006 (4)	0.424 (3)	1.0	0.005	6
O7	0.748 (4)	0.903 (5)	0.520 (4)	1.0	0.005	6
O8	0.464 (6)	0.904 (5)	0.485 (4)	1.0	0.005	6
O9	0.748 (4)	0.186 (5)	0.452 (4)	1.0	0.005	6
O10	0.717 (3)	0.657 (5)	0.749 (4)	1.0	0.005	6
(3) $Ba(Co_{0.4}Zn_{0.6})SiO_4$ ($x = 0.6$)						
Ba1	0.0	0.0	0.2434 (14)	1.0	0.002 (2)	2
Ba2	0.33333	0.66667	0.219 (2)	1.0	0.0012 (13)	2
Ba3	0.66667	0.33333	0.2180 (1)	1.0	0.019 (2)	2
Co4/Zn5	0.673 (2)	0.668 (2)	0.526 (2)	0.4/0.6	0.01	6
Si6	0.661 (3)	−0.004 (3)	0.420 (2)	1.0	0.005	6
O7	0.745 (3)	0.903 (4)	0.517 (4)	1.0	0.005	6
O8	0.468 (5)	0.895 (5)	0.475 (3)	1.0	0.005	6
O9	0.756 (4)	0.194 (5)	0.445 (3)	1.0	0.005	6
O10	0.711 (3)	0.656 (4)	0.746 (3)	1.0	0.005	6
(4) $Ba(Co_{0.2}Zn_{0.8})SiO_4$ ($x = 0.8$)						
Ba1	0.0	0.0	0.2405 (14)	1.0	0.0015 (10)	2
Ba2	0.33333	0.66667	0.219 (2)	1.0	0.0086 (14)	2
Ba3	0.66667	0.33333	0.2180 (1)	1.0	0.026 (2)	2
Co4/Zn5	0.6728 (14)	0.6678 (15)	0.527 (2)	0.2/0.8	0.01	6
Si6	0.662 (3)	−0.006 (3)	0.420 (2)	1.0	0.005	6
O7	0.751 (3)	0.900 (4)	0.516 (3)	1.0	0.005	6
O8	0.467 (4)	0.893 (4)	0.477 (3)	1.0	0.005	6
O9	0.758 (4)	0.187 (4)	0.447 (3)	1.0	0.005	6
O10	0.713 (3)	0.659 (4)	0.745 (3)	1.0	0.005	6
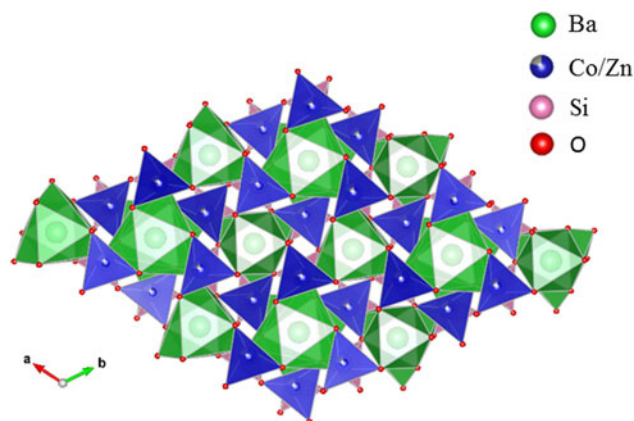
Figure 3. (Colour online) Crystal structure of $Ba(Co_{1-x}Zn_x)SiO_4$ showing corner-shared Co/ZnO_4 tetrahedra along c-axis.
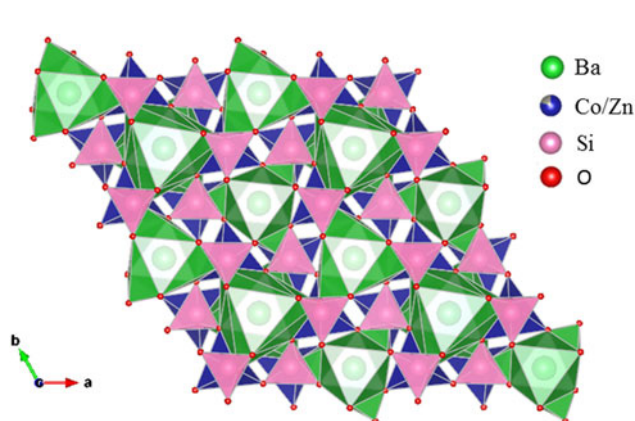
Figure 4. (Colour online) Crystal structure of $Ba(Co_{1-x}Zn_x)SiO_4$ showing corner-shared SiO_4 and the staggering larger Co/ZnO_4 tetrahedra along c-axis.
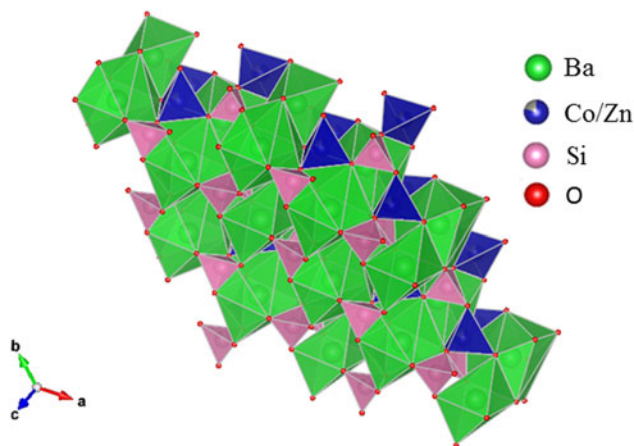
Figure 5. (Colour online) Crystal structure of $Ba(Co_{1-x}Zn_x)SiO_4$ showing the Ba polyhedra.

center in Figure 3 (coordinate *0, 0, z*), the degree of framework tilt can be estimated approximately from the difference (Δz) between the *z* coordinates of the surrounding O7 and O9 sites. The greater the Δz values, the larger the tetrahedral tilt. The Δz value was estimated to be 0.075, 0.070, 0.068, 0.072, 0.069, and 0.064 for $x = 0$, 0.2, 0.4, 0.6, 0.8 and 1.0 in $Ba(Co_{1-x}Zn_x)SiO_4$, respectively, indicating a general decrease of tetrahedral tilting. For comparison, Table V gives the values of *x*, lattice parameter *c*, Δz, and angle M-O (10)-Si in $Ba(Co_{1-x}Zn_x)SiO_4$. There is an apparent correlation between the trend of *c* parameter and the tetrahedral angle distortion (M-O(10)-Si) (deviation from the ideal angle of 109.5 °). That is, the shorter the *c* axis, the more pronounced the tetrahedral distortion.

In Table IV, the bond valence sum values around the Ba atoms in all the $Ba(Co_{1-x}Zn_x)SiO_4$ compounds are lower than the ideal value of 2.0, indicating that the Ba-O bonds are stretched, or the Ba atoms are too small relative to the size of the framework cavities. On the other hand, the SiO_4 tetrahedra are under compressive stress as their BVS values are greater than the ideal value of 4.0 (decreasing from 4.66 to 4.25 as the *x* value increases). The $(Co/Zn)O_4$ tetrahedra
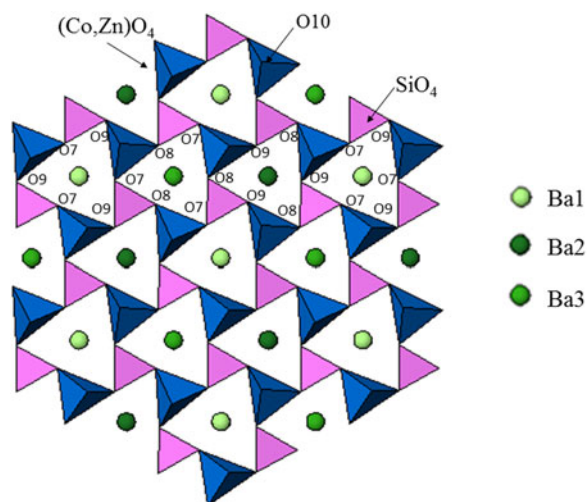

Figure 6. (Colour online) Crystal structure of $Ba(Co_{1-x}Zn_x)SiO_4$ showing the 6-membered rings with Ba atoms in the channels and the atomic labeling.

show a slight change of stress from tensile to compressive as the Zn concentration increases, parallel to the trend of decreasing average Co/Zn-O bond distances from 1.98 to 1.95 Å.

From X-ray fluorescence measurements, the atomic concentrations for Ba, Zn, Co and Si were found to be 1.00 (Normalized), 0.42 ± 0.04, 0.63 ± 0.04, and 0.76 ± 0.07, respectively. These results confirm the ratio of the concentration of Zn/Co to be of 4/6, agreeing with the chemical formula of $Ba(Zn_{0.4}Co_{0.6})SiO_4$ that we synthesized. These uncertainty estimates from our X-ray fluorescence measurements only represent the statistical, type A expanded values. This instrument will have type B expanded uncertainties of 10 to 20%, without known standards used in the quantitative measurement algorithm (No standards were used for this measurement). Si composition suffers interference with source and detector window attenuation, due to the low energy nature of its fluorescence line, which increases atomic concentration uncertainties by 20 to 30%. This could explain Si deviations from expected atomic percentages.

B. Optical properties of $Ba(Co_{1-x}Zn_x)SiO_4$

Figure 7 shows the UV-visible absorption spectra of two as-synthesized $Ba(Co_{1-x}Zn_x)SiO_4$ ($x = 0.2$ and 0.8) compounds. There is a strong absorption peak around 310 nm for $BaCo_{0.8}Zn_{0.2}SiO_4$ and 320 nm for $BaCo_{0.2}Zn_{0.8}SiO_4$. The absorption edge red-shifts with the changes of Zn content *x*.

The optical band gaps E_g can be estimated from the absorption coefficient (α) using the Tauc relation (Tauc, 1966),

$$\alpha h v = A(h v - Eg)^n$$

where *A* is a constant that depends on the transition probability, *hv* is the energy of incident photons, *n* is an index that characterizes the optical absorption process. The values of $n = 2$, 1/2, 3, and 3/2 correspond to allowed indirect, allowed direct, forbidden indirect and forbidden direct band-gap, respectively (Qasrawi, 2005). The UV-visible spectra shown in Figure 7(a) were fitted with $n = 1/2$, 2, 3, and 3/2. The value of $n = ½$ was employed in our work to calculate the band gaps. It was reported that Ba_2SiO_4 (Bispo *et al.*, 2017) and Zn_2SiO_4 (Karazhanov *et al.*, 2009) have direct transitions, in agreement with $n = 1/2$. A linear fit near the absorption edge can be achieved in the $(\alpha h v)^{1/2}$ vs. *hv* plot to calculate the allowed direct band-gap of the semiconductor material. The band gaps Eg of $Ba(Co_{1-x}Zn_x)SiO_4$ ($x = 0.2$ and 0.8) were obtained by extrapolating the linear portion of the plot to $(\alpha h v)^2 = 0$, as shown in Figure 7(b). The band gap values (allowed direct electronic transitions) are 3.47 eV for $Ba(Co_{0.8}Zn_{0.2})SiO_4$ and 3.35 eV for $Ba(Co_{0.2}Zn_{0.8})SiO_4$. The Co/Zn ratio clearly affects the band-gap value.

Theoretical calculation indicated that the band gap of $BaZnSiO_4$ to be 3.587 eV (Figure S1 in Supporting Information), close to the measured values for those in the $Ba(Co,Zn)SiO_4$ solid solution members. However, the theoretical band gap is only about 2 eV for $BaCoSiO_4$ (Taniguchi *et al.*, 2014). It appears that even with a small amount of Zn-doping, the band gap of $Ba(Co,Zn)SiO_4$ increases by a relatively large amount from 2 to 3.47 eV.

Atom	Atom	Bond distances (Å) and BVS values							
		(i) $x=0.2$	BVS	(ii) $x=0.4$	BVS	(iii) $x=0.6$	BVS	(iv) $x=0.8$	BVS
Ba1	O7 × 3	3.12 (2)	1.56	3.13 (3)	1.66	3.13 (2)	1.56	2.78 (3)	1.73
	O7 × 3	2.83 (2)		2.80 (3)		2.83 (3)		3.11 (3)	
	O10 × 3	2.92 (3)		2.89 (4)		2.92 (3)		2.88 (3)	
Ba2	O9 × 3	3.05 (3)	1.88	2.97 (4)	1.80	3.00 (3)	1.91	3.03 (4)	1.79
	O8 × 3	2.88 (2)		2.97 (4)		2.87 (3)		2.88 (3)	
	O10 × 3	2.74 (2)		2.76 (4)		2.76 (3)		2.79 (3)	
Ba3	O8 × 3	2.74 (2)	1.64	2.76 (4)	1.73	2.69 (3)	1.91	2.76 (3)	1.84
	O9 × 3	2.80 (3)		2.74 (4)		2.79 (3)		2.74 (4)	
	Ave.	2.885		2.878		2.874		2.871	
Co5/Zn5	O7	1.92 (3)	1.87	1.88 (4)	2.03	1.90 (4)	1.95	1.86 (3)	2.06
	O8	2.04 (3)		1.90 (5)		1.99 (4)		1.99 (3)	
	O9	1.94 (3)		2.06 (4)		2.02 (3)		2.01 (3)	
	O10	2.02 (2)		1.98 (2)		1.96 (2)		1.95 (2)	
	Ave.	1.98		1.96		1.97		1.95	
Si6	O7	1.53 (3)	4.67	1.64 (4)	4.25	1.63 (4)	4.30	1.67 (4)	4.27
	O8	1.65 (3)		1.65 (5)		1.60 (4)		1.61 (4)	
	O9	1.55 (3)		1.53 (4)		1.58 (4)		1.54 (4)	
	O10	1.55 (2)		1.60 (3)		1.58 (2)		1.59 (2)	
	Ave (Si-O)	1.57		1.61		1.60		1.60	

The ideal BVS values are 2.0 (Ba site), 2.0 (mixed Co/Zn site), and 4.0 (Si site), respectively. The values for the reference distance R_0 for Ba-O, Zn^{2+}-O, Co^{2+}-O, Si^{4+}-O are 2.29, 1.704, 1.692, 1.624, respectively (Brown and Altermatt, 1985; and Brese and O'Keeffe, 1991).

From the simulation and experimental measurements, it is clear that the Ba(Co$_{1-x}$Zn$_x$)SiO$_4$ ($x=0.2$–0.8) have wide band gaps over 3.3 eV, and only absorb UV portion of the solar radiation. Therefore, the Ba(Co$_{1-x}$Zn$_x$)SiO$_4$ ($x=0.2$–0.8) materials are potential UV photocatalysts. In order to obtain photocatalytic Ba(Co$_{1-x}$Zn$_x$)SiO$_4$ materials which absorb visible light, the Zn content should be lower.

The photoluminescence (PL) emission spectra of Ba(Co$_{1-x}$Zn$_x$)SiO$_4$ are shown in Figure 8. The spectra show broad and intense emission extending to the IR range. Similar to Ba$_2$SiO$_4$ with a wide band gap (Zhang *et al.*, 2007; Bispo *et al.*, 2017), the materials are expected to be suitable for a color converter and solid-state lighting using UV light as an excitation source. It should be noted that the Co/Zn ratio does not affect the main emission peak at 543 nm significantly.

C. Reference powder X-ray diffraction patterns

Reference patterns for Ba(Co$_{1-x}$Zn$_x$)SiO$_4$ ($x=0.2$, 0.4, 0.6, 0.8) have been prepared and submitted for inclusion in the PDF. An example of the pattern Ba(Co$_{0.6}$Zn$_{0.4}$)SiO$_4$ is given in Table VI. In this pattern, the symbols "M" and "+" refer to peaks containing contributions from two and more

TABLE V. Values of x, c, Δz and angle M-O(10)-Si in Ba(Co$_{1-x}$Zn$_x$)SiO$_4$, where M represents the mixed sites of Co/Zn. Δz represents the difference between the z-coordinate of O7 and O9.

x	c	Δz (Å)	M-O(10)-Si (°)	Reference
0.0	8.6818 (10)	0.075	148.6	Liu and Barbier, (1993)
0.2	8.69477 (12)	0.070	149.8 (11)	This work
0.4	8.70614 (13)	0.068	149.3 (13)	This work
0.6	8.71363 (12)	0.072	151.2 (12)	This work
0.8	8.72200 (10)	0.069	152.2 (11)	This work
1.0	8.7147 (11)	0.064	156.1	Liu and Barbier, (1993)

than two reflections, respectively. The particular peak that has the strongest intensity in the entire pattern is assigned an intensity of 999 and other lines are scaled relative to this value. In general, the d-spacing values are calculated values from refined lattice parameters. The intensity values reported are integrated intensities (rather than peak heights). For resolved overlapped peaks, intensity-weighted calculated d-spacing, along with the observed integrated intensity and the *hkl* indices of both peaks (for "M"), or the *hkl* indices of the strongest peak (for "+") are used. For peaks that are not resolved at the instrumental resolution, the intensity-weighted average d-spacing and the summed integrated intensity value are used. In the case of a cluster, unconstrained profile fits often reveal the presence of multiple peaks, even when they are closer than the instrumental resolution. In this situation, both d-spacing and intensity values are reported independently.

IV. SUMMARY

Ba(Co$_{1-x}$Zn$_x$)SiO$_4$ belong to the large structural family of stuffed-tridymite (SiO$_2$). Crystal structure and reference patterns of the Ba(Co$_{1-x}$Zn$_x$)SiO$_4$ ($x=0.2$, 0.4, 0.6, 0.8) series of compounds have been determined. From powder X-ray diffraction studies, Ba(Co$_{1-x}$Zn$_x$)SiO$_4$ adopts a simple hexagonal structure with $P6_3$ space group (No. 173), with $Z=6$. There are three crystallographically independent Ba sites; two nine-fold coordinated and one six-fold sites. The ionic radii of Zn^{2+} and Co^{2+} are very similar, resulting in the similarity of the unit cell volume of the solid solution members. The structure consists of fully ordered corner-shared SiO$_4$ and (Co/Zn)O$_4$ tetrahedra. Band gap measurements using UV-visible absorption spectroscopy confirm the band gaps of Ba(Co$_{1-x}$Zn$_x$)SiO$_4$ materials to be too wide to be useful as photocatalysis materials in the visible light range, but as potential UV photocatalysts. Powder X-ray diffraction patterns of these compounds have been

TABLE VI. X-ray powder pattern for Ba(Co$_{0.6}$Zn$_{0.4}$)SiO$_4$ ($P6_3$ (No. 173), $Z = 6$, 9.11386(8) Å, $c = 8.70614(13)$ Å, $V = 626.269(11)$ Å^3, $D_x = 4.628$ g.cm^{-3}).

d_{cal}	I_{obs}	h	k	l	d_{cal}	I_{obs}	h	k	l	d_{cal}	I_{obs}	h	k	l
7.8929	3	0	1	0	4.5569	195	1	1	0	4.3530	12	0	0	2
4.0373	123	1	1	1	3.8118	5	0	1	2	3.1477	999	1	1	2
2.9832	4	2	1	0 M	2.9832	4	1	2	0 M	2.9238	7	0	2	2
2.7238	1	0	1	3	2.6310	485	0	3	0	2.5185	30	0	3	1
2.4608	16	1	2	2 M	2.4608	16	2	1	2 M	2.4478	53	1	1	3
2.2785	54	2	2	0	2.2517	108	0	3	2	2.2042	38	2	2	1
2.1765	99	0	0	4	2.1230	6	3	1	1 M	2.1230	6	1	3	1 M
2.0982	19	0	1	4	2.0187	274	2	2	2	1.9640	128	1	1	4
1.9492	13	0	3	3	1.9059	5	0	2	4	1.7921	23	2	2	3
1.7583	4	2	1	4	1.7224	42	1	4	0 M	1.7224	42	4	1	0 M
1.6896	24	4	1	1 M	1.6896	24	1	4	1 M	1.6770	135	0	3	4
1.6265	49	1	1	5	1.6016	261	1	4	2 M	1.6016	261	4	1	2 M
1.5738	67	2	2	4	1.5435	16	3	1	4 M	1.5435	16	1	3	4 M
1.5190	134	3	3	0	1.4916	2	2	4	0	1.4840	2	0	5	2
1.4811	35	1	4	3 M	1.4811	35	4	1	3 M	1.4619	4	0	4	4
1.4510	11	0	0	6	1.4342	3	3	3	2	1.4271	3	0	1	6
1.4111	1	2	4	2	1.3920	4	3	2	4	1.3830	54	2	2	5 M
1.3830	54	1	1	6 M	1.3627	3	1	3	5	1.3506	73	1	4	4 M
1.3506	73	4	1	4 M	1.3266	1	4	2	3	1.3155	52	0	6	0
1.3049	17	2	1	6 M	1.3049	17	2	1	6 M	1.3007	2	0	6	1
1.2834	1	4	3	1	1.2706	70	0	3	6	1.2639	15	5	2	0 M
1.2639	15	2	5	0 M	1.2592	12	0	6	2	1.2551	1	3	2	5
1.2508	3	2	5	1 M	1.2508	3	5	2	1 M	1.2456	65	3	3	4
1.2304	7	2	4	4 M	1.2304	7	4	2	4 M	1.2243	47	2	2	6 +
1.2137	114	5	2	2 M	1.2137	114	2	5	2 M	1.2094	4	1	3	6 M
1.2094	4	3	1	6 M	1.1998	8	1	1	7	1.1879	4	5	1	4 M
1.1879	4	1	5	4 M	1.1588	8	5	2	3 M	1.1588	8	2	5	3 M
1.1392	2	4	4	0	1.1323	4	2	3	6 M	1.1323	4	3	2	6 M
1.1258	27	0	6	4	1.1145	4	4	3	4 M	1.1145	4	3	4	4 M
1.1097	27	4	1	6 M	1.1097	27	1	4	6 M	1.1021	38	4	4	2
1.0930	31	2	5	4 M	1.0930	31	5	2	4 M	1.0917	4	2	2	7
1.0781	4	0	1	8	1.0683	4	0	5	6	1.0604	4	4	4	3
1.0585	24	1	1	8	1.0533	2	6	1	4	1.0492	21	3	3	6
1.0454	9	7	1	0 M	1.0454	9	1	7	0 M	1.0401	4	2	4	6
1.0228	12	2	5	5 M	1.0228	12	5	2	5 M	1.0165	46	1	7	2 M
1.0165	46	7	1	2 M	1.0093	10	4	4	4	1.0083	6	4	1	7 M
1.0083	6	1	4	7 M	1.0012	2	0	7	4	0.9944	36	3	6	0 M
0.9944	36	6	3	0 M	0.9836	7	7	1	3 M	0.9836	7	1	7	3 M
0.9820	17	2	2	8	0.9746	25	0	6	6 +	0.9694	6	6	3	2 M
0.9694	6	3	6	2 M	0.9530	15	2	5	6 M	0.9530	15	5	2	6 M
0.9424	16	7	1	4 M	0.9424	16	1	7	4 M	0.9328	3	3	2	8 M
0.9328	3	2	3	8 M	0.9264	1	6	1	6	0.9200	24	1	4	8 M
0.9200	24	4	1	8 M	0.9114	2	5	5	0	0.9045	22	6	3	4 M
0.9045	22	3	6	4 M	0.8962	11	4	4	6 +	0.8920	14	5	5	2
0.8903	3	3	5	6 M	0.8903	3	5	3	6 M	0.8865	3	2	5	7 M
0.8865	3	5	2	7 M	0.8847	1	3	3	8	0.8816	1	2	7	4
0.8792	2	4	2	8 M	0.8792	2	2	4	8 M	0.8770	10	0	9	0
0.8738	3	6	2	6 M	0.8738	3	2	6	6 M	0.8706	3	0	0	10
0.8695	1	5	5	3	0.8654	2	0	1	10	0.8632	4	5	1	8 M
0.8632	4	1	5	8 M	0.8612	4	8	2	0 M	0.8612	4	2	8	0 M
0.8597	1	0	9	2	0.8551	1	1	1	10	0.8503	2	1	8	4 M
0.8503	2	0	2	10M	0.8482	8	7	1	6 M	0.8482	8	1	7	6 M
0.8448	20	8	2	2 M	0.8448	20	2	8	2 M	0.8407	6	5	5	4
0.8358	4	2	1	10M	0.8356	4	1	2	10M	0.8338	4	3	4	8 M
0.8338	4	4	3	8 M	0.8293	3	4	5	6 M	0.8293	3	5	4	6 M
0.8265	13	0	3	10	0.8247	15	5	2	8 M	0.8247	15	2	5	8 M
0.8222	2	3	7	4 M	0.8222	2	7	3	4 M	0.8203	16	3	6	6 M
0.8203	16	6	3	6 M	0.8184	4	4	7	0 M	0.8184	4	7	4	0 M
0.8159	1	0	8	6	0.8134	10	0	9	4	0.8090	4	1	3	10M
0.8090	4	3	1	10M	0.8072	3	1	6	8 M	0.8072	3	6	1	8 M
0.8044	15	4	7	2 M	0.8044	15	7	4	2 M	0.8008	9	2	8	4 M
0.8008	9	8	2	4 M	0.7965	1	0	4	10	0.7869	6	4	4	8
0.7846	2	3	2	10M	0.7846	2	2	3	10M	0.7793	2	8	1	6
0.7719	5	5	5	6 +	0.7661	6	4	7	4 M	0.7661	6	7	4	4 M
0.7624	1	0	5	10	0.7595	6	6	6	0	0.7554	7	3	3	10
0.7539	9	1	7	8 M	0.7539	9	7	1	8 M	0.7519	2	2	4	10

Continued

TABLE VI. Continued

d_{cal}	I_{obs}	h	k	l	d_{cal}	I_{obs}	h	k	l	d_{cal}	I_{obs}	h	k	l
0.7506	4	0	9	6	0.7419	2	1	5	10M	0.7419	2	5	1	10M
0.7406	7	8	2	6 +	0.7383	10	1	10	2 M	0.7383	10	10	1	2 M
0.7297	8	3	9	0 M	0.7297	8	9	3	0 M	0.7260	6	0	6	10
0.7171	3	6	6	4	0.7165	2	1	1	12	0.7129	3	7	4	6 M
0.7129	3	4	7	6 M	0.7084	3	1	10	4 M	0.7084	3	10	1	4 M
0.6919	5	3	9	4 M	0.6919	5	9	3	4 M	0.6913	2	2	2	12
0.6862	8	5	8	2 M	0.6862	8	8	5	2 M	0.6753	5	2	8	8 M
0.6753	5	8	2	8 M	0.6729	2	6	6	6	0.6550	7	3	6	10M
0.6550	7	6	3	10M	0.6519	4	3	9	6 M	0.6519	4	9	3	6 M
0.6438	8	2	11	2 +	0.6296	2	0	12	4	0.6254	3	10	4	2 M
0.6254	3	4	10	2 M	0.6175	4	0	9	10+					

The symbols "M" and "+" refer to peaks containing contributions from two and more than two reflections, respectively. The particular peak that has the strongest intensity in the entire pattern is assigned an intensity of 999 and other lines are scaled relative to this value. The d-spacing values are calculated values from refined lattice parameters, and "I" represents integrated intensity values.
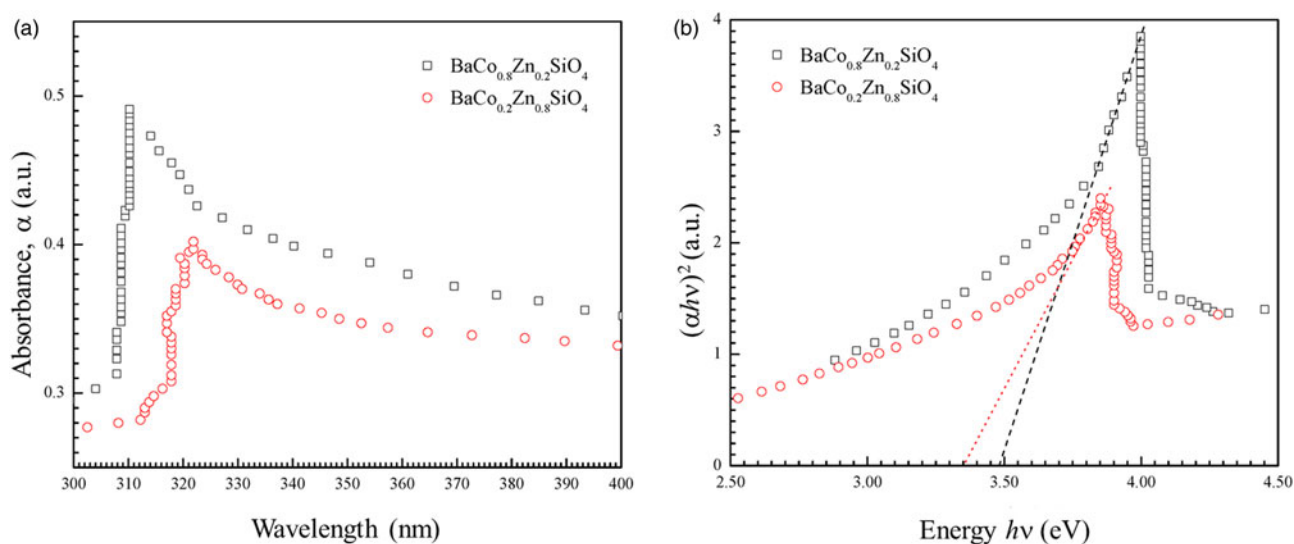

Figure 7. (Colour online) (a) UV-visible absorption spectra of the as-synthesized $Ba(Co_{0.8}Zn_{0.2})SiO_4$ and $Ba(Co_{0.2}Zn_{0.8})SiO_4$ suspending in water. (b) Tauc plot for calculating band gaps Eg of $Ba(Co_{0.8}Zn_{0.2})SiO_4$ and $Ba(Co_{0.2}Zn_{0.8})SiO_4$ by extrapolation of the linear portion of the plots of $(\alpha h\nu)^2$ vs. $h\nu$.
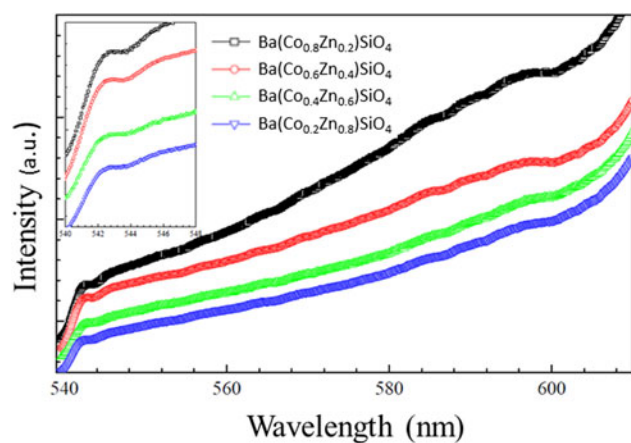

Figure 8. (Colour online) Photoluminescence (PL) emission spectra of Ba$(Co_{1-x}Zn_x)SiO_4$ under 502 nm excitation. Inset: Zoomed spectrum from 540 to 548 nm for details.

submitted to be included in the Powder Diffraction File (PDF).

SUPPLEMENTARY MATERIAL

To view supplementary material for this article, please visit https://doi.org/10.1017/S0885715619000447

Abe, R. (**2010**). "Recent progress on photocatalytic and photoelectrochemical water splitting under visible light irradiation," J. Photochem. Photobiol. C Photochem. Rev. **11**, 179–209.

Barry, T. L. (**1968**). "Fluorescence of Eu-activated phases in binary alkaline earth orthosilicate systems," J. Electrochem. Soc. **115**, 1181–1184.

Bispo, A. G. Jr, Ceccato, D. A., Lima, S. A. M., and Pires, A. M. (**2017**). "Red phosphor based on Eu^{3+}-isoelectronically doped Ba_2SiO_4 obtained via sol–gel route for solid state lightning," RSC Adv. **7**, 53752.

Brese, N. E. and O'Keeffe, M. (**1991**). "Bond-valence parameters for solids," Acta Crystallogr. B **47**, 192–197.

Brown, I. D. and Altermatt, D. (**1985**). "Bond-valence parameters obtained from a systematic analysis of the Inorganic Crystal Structure Database," Acta Crystallogr. B **41**, 244–247.

Jüstel, H., Nikol, H., and Ronda, C. (**1998**). "New developments in the field of luminescent materials for lighting and displays," Angew Chem. Int. Ed. **37**, 3048.

Karazhanov, S. Z., Ravindran, P., Fjellvåg, H., and Svensson, B. G. (**2009**). "Electronic structure and optical properties of $ZnSiO_3$ and Zn_2SiO_4," J. Appl. Phys. **106**, 123701.

Khan, M. M., Adil, S. F., and Al-Mayouf, A. (**2015**) "Metal oxides as photocatalysts," J. Saudi Chemical Soc. **19**, 4620464.

King, N., Boltersdorf, J., Maggard, P., and Wong-Ng, W. (**2017**). "Polymorphism and structural distortions of ternary mixed-metal oxide photocatalysts constructed with α-U_3O_8 types of layers," Crystals. (Basel) **7**, 145.

Larson, A. C., and von Dreele, R. B. (**2004**). *General Structure Analysis System (GSAS)*, Los Alamos National Laboratory Report LAUR 86-748, Los Alamos, USA.

Lin, Y., Niu, Z., Han, Y., Li, C., Zhou, W., Zhang, J., Yu, L., and Lian, S. (**2017**). "The self-reduction ability of RE^{3+} in orthosilicate (RE = Eu, Tm, Yb, Sm): $BaZnsiO_4$-based phosphorus prepared in air and its luminescence," J. Alloys and Comp. **690**, 267–273.

Liu, B., and Barbier, J. (**1993**). "Structures of the Stuffed Tridymite Derivative, $BaMSiO_4$ (M = Co, Zn, Mg)," J. Solid State Chem. **102**, 115–125.

Maeda, K. (**2011**). "Photocatalytic water splitting using semiconductor particles: history and recent developments," J. Photochem. Photobiol. C Photochem. Rev. **12**, 237–268.

Martsinovich, N. (**2016**). "Theory of materials for solar energy conversion," J. Phys. Condens. Matter **28**, 70301.

McMurdie, H. F., Morris, M. C., Evans, E. H., Paretzkin, B., and Wong-Ng, W. (**1986a**). "Methods of producing standard Xray diffraction powder patterns," Powder Diffr. **1**(1), 40.

McMurdie, H. F., Morris, M. C., Evans, E. H., Paretzkin, B., Wong-Ng, W., Ettlinger, L., and Hubbard, C. R. (**1986b**). "JCPDS—international Centre for Diffraction Data task group on cell parameter refinement," Powd. Diffr. **1**(2), 66–76.

Nagai, T., Asai, S., Okazaki, R., Terasaki, I., and Taniguchi, H. (**2015**). "Effects of element substitution on the pyroelectric phase transition of stuffed-tridymite-type $BaZnGeO_4$," Solid State. Comm. **219**, 12–15.

Osterloh, F. E. (**2013**). "Inorganic nanostructures for photoelectrochemical and photocatalytic water splitting," Chem. Soc. Rev. **42**, 2294–2320.

Paranthaman, M. P., Wong-Ng, W., and Bhattacharya, RN. (**2015**). "Semiconductor Materials for Solar Photovoltaic (PV) Cells," Springer Series in Materials Science 218, Springer US, New York, New York.

PDF4+ (**2019**) (Database), edited by Dr. Soorya Kabekkodu, International Centre for Diffraction Data, Newtown Square, PA, 19073-3273, USA.

Qasrawi, A. F. (**2005**). "Refractive index, band gap and oscillator parameters of amorphous GaSe thin films," Cryst. Res. Technol., **40**(6), 610–614..

Rietveld, H. M. (**1969**) "A profile refinement method for nuclear and magnetic structures," J. Appl. Cryst. **2**, 65–71.

Shannon, R. D. (**1976**). "Revised effective ionic radii and systematic studies of interatomic distances in halides and chalcogenides," Acta Crystallogr. **A32**, 751–767.

Streit, H. C., Kramer, J., Suta, M., and Wickleder, C. (**2013**). "Red, green, and blue photoluminescence of Ba_2SiO_4:M (M = Eu^{3+}, Eu^{2+}, Sr^{2+}) Nanophosphors," Materials **6**, 3079–3093.

Taniguschi, H., Moriwake, H., Kuwabara, A., Okamura, T., Yamamoto, T., Okazaki, R., Itoh, M., and Terasaki, I. (**2014**). "Photo-induced change of dielectric response in $BaCoSiO_4$ stuffed tridymite," J. Appl. Phys. **115**, 164103.

Tauc, J., Grigorovici, R., and Vancu, A. (**1966**). "Optical properties and electronic structure of amorphous germanium," Physica Status Solidi (b) **15** (2), 627–637.

Yao, S.-S., Xue, L.-H., and Yan, Y.-W. (**2011**). "Synthesis and luminescent properties of hexagonal $BaZnSiO_4$:Eu^{2+} phosphor," Appl. Phys. B **102**, 705–709.

Zhang, M., Wang, J., Zhang, Q., Ding, W., and Su, Q. (**2007**). "Optical properties of Ba_2SiO_4:Eu^{2+} phosphor for green light-emitting diode (LED)," Mater. Res. Bull. **42**, 33–39.